

## Short communication

# Microstructure and dielectric tunable properties of $\text{SrO}(\text{Sr}_{1-x}\text{Ba}_x\text{TiO}_3)_n$ microwave ceramics

Jiangying Wang<sup>\*</sup>, Huang Zhou, Jintao Liu, Shengyong Jin, Lina Sun, Jingji Zhang

*College of Materials Science and Engineering, China Jiliang University, Hangzhou 310018, China*

Received 13 December 2011; received in revised form 14 December 2011; accepted 15 December 2011

Available online 23 December 2011

## Abstract

Microstructure and dielectric tunable properties of  $\text{SrO}(\text{Sr}_{1-x}\text{Ba}_x\text{TiO}_3)_n$  ( $x = 0$  and  $0.5$ ,  $n = 1-4$ ) microwave ceramics prepared through solid-state reactions have been investigated. For  $\text{SrO}(\text{SrTiO}_3)_n$  series,  $\text{Sr}_2\text{TiO}_4$  can be isolated as single phase in  $n = 1$  product and  $\text{Sr}_4\text{Ti}_3\text{O}_{10}$  appears in the  $n \geq 2$  cases as either a major phase ( $n = 3, 4$ ) or a second phase ( $n = 2$ ).  $\text{Ba}^{2+}$  substitution for  $\text{Sr}^{2+}$  causes the formation of  $\text{SrTiO}_3$  and  $\text{Ba}_x\text{Sr}_{2-x}\text{TiO}_4$ .  $\text{SrO}(\text{Sr}_{1-x}\text{Ba}_x\text{TiO}_3)_n$  ( $n = 1, 2$ ) have no dielectric non-linear behavior in the temperature range of  $-165$  to  $50$  °C. As  $n$  increases, the tunability increases. As a result,  $\text{Ba}^{2+}$  substitution for  $\text{Sr}^{2+}$  results in an increase in permittivity and tunability, but a decrease in  $Q$  value. © 2011 Elsevier Ltd and Techna Group S.r.l. All rights reserved.

**Keywords:** Layered perovskite structure; Tunability; Microwave properties

## 1. Introduction

$\text{SrO}(\text{SrTiO}_3)_n$  ( $n = \text{integer}$ ) series represents the prototype of a huge family of layered oxides described by Ruddlesden and Popper [1,2], consisting of alternate stacks of SrO layers and perovskite ( $\text{SrTiO}_3$ )<sub>*n*</sub> block layers along the *c*-axis. The upper member of  $\text{SrO}(\text{SrTiO}_3)_n$  is the well-known  $\text{SrTiO}_3$  ( $n = \infty$ ), which has been commonly used in grain boundary barrier-layer capacitors [3], resistive oxygen gas-sensors [4], solar cells [5], solid oxide electronic devices [6,7], substrates for perovskite films [8], and efficient photocatalysts [9,10]. The properties of  $\text{SrO}(\text{SrTiO}_3)_n$  have yet been fully explored. They are expected to have applications like  $\text{SrTiO}_3$ .

Strained  $\text{SrTiO}_3$  can exhibit ferroelectricity even at room temperature [11]. The relatively high tunability of the strained  $\text{SrTiO}_3$  unfortunately signifies a remarkable increase in both relative permittivity and loss, rendering it less useful for high-frequency applications. The prospect of “engineering” the properties of  $\text{SrO}(\text{SrTiO}_3)_n$  by varying  $n$  has stimulated experimental research as well as theoretical studies [12,13]. Its relative permittivity decreases as  $n$  decreases [14].  $\text{SrO}(\text{SrTiO}_3)_n$  may provide new tunable materials which have

decreased loss [15]. Wise et al. [14] found that  $(\text{Sr}_x\text{Ca}_{1-x})_{n+1} + 1\text{Ti}_n\text{O}_{3n+1}$  exhibited higher quality factors ( $Q = 1/\tan \delta$ ) than  $\text{Sr}_{n+1}\text{Ti}_n\text{O}_{3n+1}$ . This paper was aimed to study dielectric properties of  $\text{SrO}(\text{Sr}_{1-x}\text{Ba}_x\text{TiO}_3)_n$  ( $x = 0$  and  $0.5$ ,  $n = 1-4$ ) ceramics.

## 2. Experimental procedure

$\text{SrO}(\text{Sr}_{1-x}\text{Ba}_x\text{TiO}_3)_n$  ( $x = 0$  and  $0.5$ ,  $n = 1-4$ ) ceramics were prepared through the conventional solid-state reaction method. High-purity  $\text{BaCO}_3$  (99.0%, Sinopharm Chemical Reagent Co., Ltd., China),  $\text{SrCO}_3$  (99.0%, Sinopharm Chemical Reagent Co., Ltd., China) and  $\text{TiO}_2$  (98.0%, Sinopharm Chemical Reagent Co., Ltd., China) powders were used as starting materials. Mixtures based on the compositions of  $\text{SrO}(\text{Sr}_{1-x}\text{Ba}_x\text{TiO}_3)_n$  ( $x = 0$  and  $0.5$ ,  $n = 1-4$ ) were ball-milled with zirconia media in ethanol for 24 h and then dried at  $110$  °C for 12 h. After drying, the powders were calcined at  $1200$  °C for 4 h and then re-milled for 24 h. The calcined powders, mixed with 8 wt% polyvinyl alcohol (PVA), were pressed into pellets at 100 MPa. The green pellets were kept at  $550$  °C for 6 h to remove the solvent and the binder.  $\text{SrO}(\text{SrTiO}_3)_n$  and  $\text{SrO}(\text{Sr}_{0.5}\text{Ba}_{0.5}\text{TiO}_3)_n$  ceramics were sintered for 5 h in air at  $1500$  °C and  $1450$  °C, respectively.

Phase compositions of the ceramics were investigated by means of X-ray diffraction (XRD, Bruker D8 Advanced,

<sup>\*</sup> Corresponding author. Tel.: +86 571 86875609.

E-mail address: [wjyliu@163.com](mailto:wjyliu@163.com) (J. Wang).

Germany) with  $\text{CuK}\alpha$  radiation. Microstructural information was obtained by using a scanning electron microscopy (SEM, JSM EMP-800). Permittivity as a function of temperature was measured at 10 kHz in the temperature range of  $-165$  to  $50^\circ\text{C}$ , under 0 kV/cm and 30 kV/cm, respectively, using a Keithley model 2410 (Cleveland, OH) high-voltage source, coupled with TH2816A LCR meter (Changzhou, China). Permittivity and loss tangent at microwave frequencies was measured by the Hakki-Coleman dielectric resonator method, using a network analyzer (AV 3629A) in combination with a resonating cavity [16].

### 3. Results and discussion

XRD patterns of the  $\text{SrO}(\text{SrTiO}_3)_n$  ( $n = 1-4$ ) ceramics are shown in Fig. 1(a). For the sample with  $n = 1$ ,  $\text{Sr}_2\text{TiO}_4$  can be

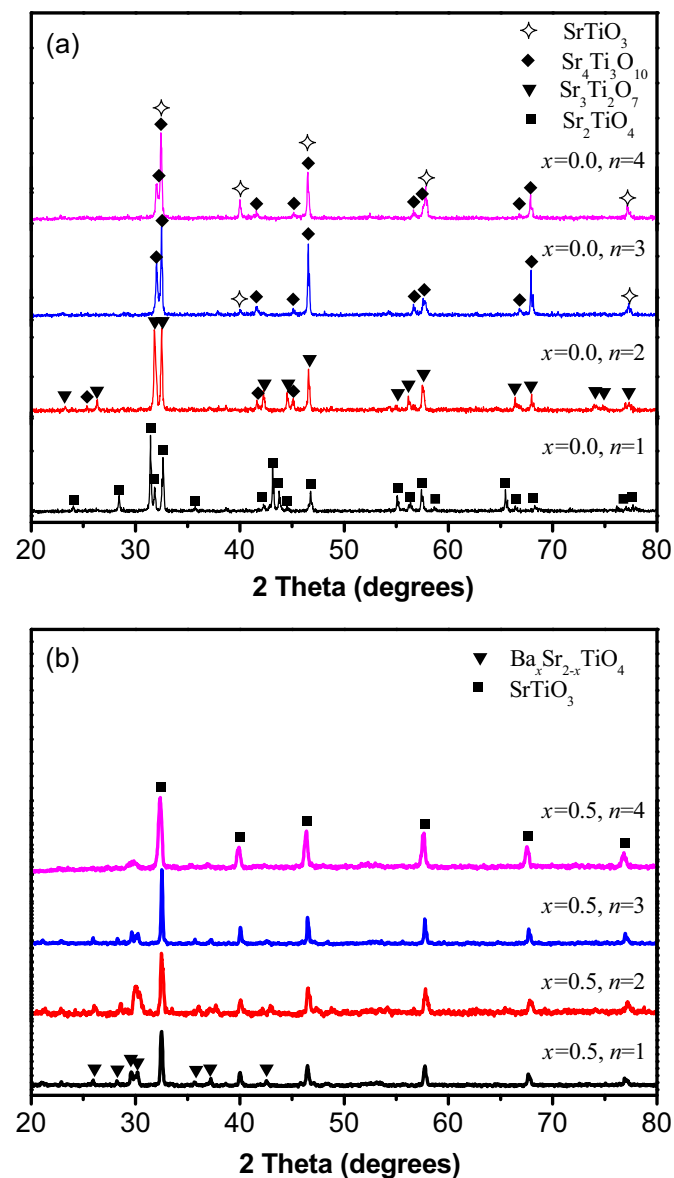


Fig. 1. XRD patterns of the  $\text{SrO}(\text{Sr}_{1-x}\text{Ba}_x\text{TiO}_3)_n$  ( $x = 0.0$  and  $0.5$ ,  $n = 1-4$ ) ceramics: (a)  $x = 0.0$  and (b)  $x = 0.5$ .

isolated as single phase according to JCPDF Nos. 72-2040 and 72-2041.  $\text{Sr}_4\text{Ti}_3\text{O}_{10}$  appears in the samples with  $n \geq 2$  as either a major phase ( $n = 3$  and  $4$ ) or a second phase ( $n = 2$ ). Wise et al. [14] reported that  $\text{Sr}_3\text{Ti}_2\text{O}_7$  appeared in all samples as either a major phase ( $n \geq 2$ ) or a second phase ( $n = 1$ ). It can be seen that  $\text{SrTiO}_3$  diffraction peaks appear in the sample with  $n = 3$  and become stronger as  $n$  increases, which is in agreement with the results reported by Wise et al. [14].

Fig. 1(b) shows XRD patterns of the  $\text{SrO}(\text{Sr}_{0.5}\text{Ba}_{0.5}\text{TiO}_3)_n$  ( $n = 1-4$ ) samples. All members have additional diffraction lines besides  $\text{SrTiO}_3$  peaks, which can be assigned to  $\text{Ba}_x\text{Sr}_{2-x}\text{TiO}_4$  [17]. It means that  $\text{Ba}_x\text{Sr}_{2-x}\text{TiO}_4$  is more stable than  $\text{Ba}_x\text{Sr}_{1-x}\text{TiO}_3$ . Meanwhile, it is notable that the  $\text{Ba}_x\text{Sr}_{2-x}\text{TiO}_4$  diffraction peaks become weaker as  $n$  increases. According to Wise et al. [14],  $(\text{Sr}_x\text{Ca}_{1-x})_3\text{Ti}_2\text{O}_7$  could be single phase. Single phase  $(\text{Sr}_x\text{RE}_{1-x})_3\text{Ti}_2\text{O}_7$  ceramics were also reported by Wang et al. [18,19]. Here,  $(\text{Sr}_x\text{Ba}_{1-x})_3\text{Ti}_2\text{O}_7$  was not formed, which may be attributed to the destroyed symmetry of  $\text{TiO}_6$  by the substitution for  $\text{Sr}^{2+}$  with larger  $\text{Ba}^{2+}$ . Wang et al. found that higher symmetry of  $\text{TiO}_6$  was achieved by the substitution for  $\text{Sr}^{2+}$  with smaller  $\text{RE}^{2+}$  [20].

As shown in Fig. 2, the  $n = 1$  and  $n = 2$  samples have homogeneous microstructure with grains of  $2-10\ \mu\text{m}$ , while the  $n = 3$  and  $4$  samples have a bimodal microstructure, consisting of pellet-shaped grains with a size of  $\sim 50\ \mu\text{m}$  and fine grains of  $2-10\ \mu\text{m}$ . Block-like grains and porous microstructures are observed in  $n = 3$  and  $n = 4$  samples because the migration of grain boundaries was hindered during sintering [21].

Fig. 3 shows SEM image of the  $\text{SrO}(\text{Sr}_{0.5}\text{Ba}_{0.5}\text{TiO}_3)_n$  ( $n = 1-4$ ) ceramics. The  $\text{SrO}(\text{Sr}_{0.5}\text{Ba}_{0.5}\text{TiO}_3)_n$  ceramics except that with  $n = 1$  have quite dense microstructure. The  $n = 1$  sample has a bimodal microstructure, consisting of vermiculate-shaped grains of  $2-5\ \mu\text{m}$ , and platelet grains with a size of  $\sim 8\ \mu\text{m}$ , whereas the  $n \geq 2$  samples have a homogeneous microstructure. Compared to  $\text{SrO}(\text{SrTiO}_3)_n$  ( $n \geq 3$ ), the  $\text{SrO}(\text{Sr}_{0.5}\text{Ba}_{0.5}\text{TiO}_3)_n$  ( $n \geq 3$ ) ceramics has no platelet grains, possibly due to the formation of an orthorhombic  $\text{Ba}_2\text{TiO}_4$ -type structure [17].

Similar to that of quantum paraelectric  $\text{SrTiO}_3$ , Curie temperature of the  $\text{SrO}(\text{SrTiO}_3)_n$  sample is also very low ( $< -165^\circ\text{C}$ ). Temperature-permittivity curves of the  $\text{SrO}(\text{Sr}_{1-x}\text{Ba}_x\text{TiO}_3)_n$  ( $x = 0.0$  and  $0.5$ ,  $n = 1, 2$ ) ceramics measured at 30 kV/cm are almost identical to those at 0 kV/cm, indicating that their tunabilities are almost zero in the temperature range of  $-165$  to  $50^\circ\text{C}$ . Temperature dependencies of permittivity of the  $\text{SrO}(\text{Sr}_{1-x}\text{Ba}_x\text{TiO}_3)_n$  ( $x = 0.0$  and  $0.5$ ,  $n = 3, 4$ ) ceramics, measured at 0 kV/cm and 30 kV/cm, are displayed in Fig. 4. Calculated tunabilities at  $-150^\circ\text{C}$  and  $-100^\circ\text{C}$  are listed in Table 1. The increase in tunability of the  $\text{SrO}(\text{SrTiO}_3)_n$  ceramics with increasing  $n$  is due to the increase in  $\text{TiO}_6$  content. The tunability at  $-150^\circ\text{C}$  of the  $\text{SrO}(\text{Sr}_{0.5}\text{Ba}_{0.5}\text{TiO}_3)_n$  samples markedly increases as compared to that of the  $\text{SrO}(\text{SrTiO}_3)_n$  ceramics, whereas their tunabilities at  $-100^\circ\text{C}$  are almost the same, suggesting the formation of  $\text{Ba}_x\text{Sr}_{2-x}\text{TiO}_4$  instead of  $\text{Ba}_x\text{Sr}_{1-x}\text{TiO}_3$  [22]. The tunability of the  $\text{SrO}(\text{Sr}_{1-x}\text{Ba}_x\text{TiO}_3)_n$  ( $x = 0.0$  and  $0.5$ ,  $n = 3, 4$ ) ceramics decreases with increasing temperature, which is attributed to

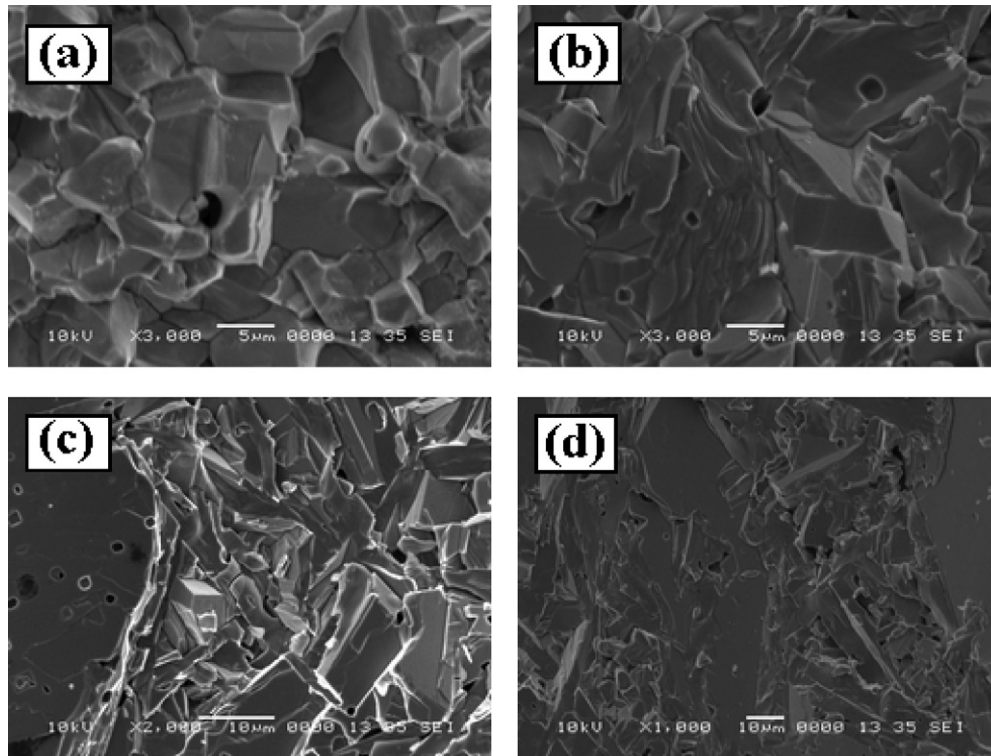


Fig. 2. Cross-section SEM images of the  $\text{SrO}(\text{SrTiO}_3)_n$  ceramics: (a)  $n = 1$ , (b)  $n = 2$ , (c)  $n = 3$  and (d)  $n = 4$ .

the fact that residual polar/distorted clusters are absent when the temperature is far beyond Curie temperature.

Microwave dielectric parameters of the  $\text{SrO}(\text{Sr}_{1-x}\text{Ba}_x\text{TiO}_3)_n$  ( $x = 0.0$  and  $0.5$ ,  $n = 1-4$ ) ceramics are also listed in Table 1.

For the  $\text{SrO}(\text{SrTiO}_3)_n$  series, permittivity increases with increasing  $n$ , whereas  $Q$  value slightly decreases. Structurally, both permittivity and  $Q$  value of a material depend on its composition and crystal structure. For microwave dielectrics,

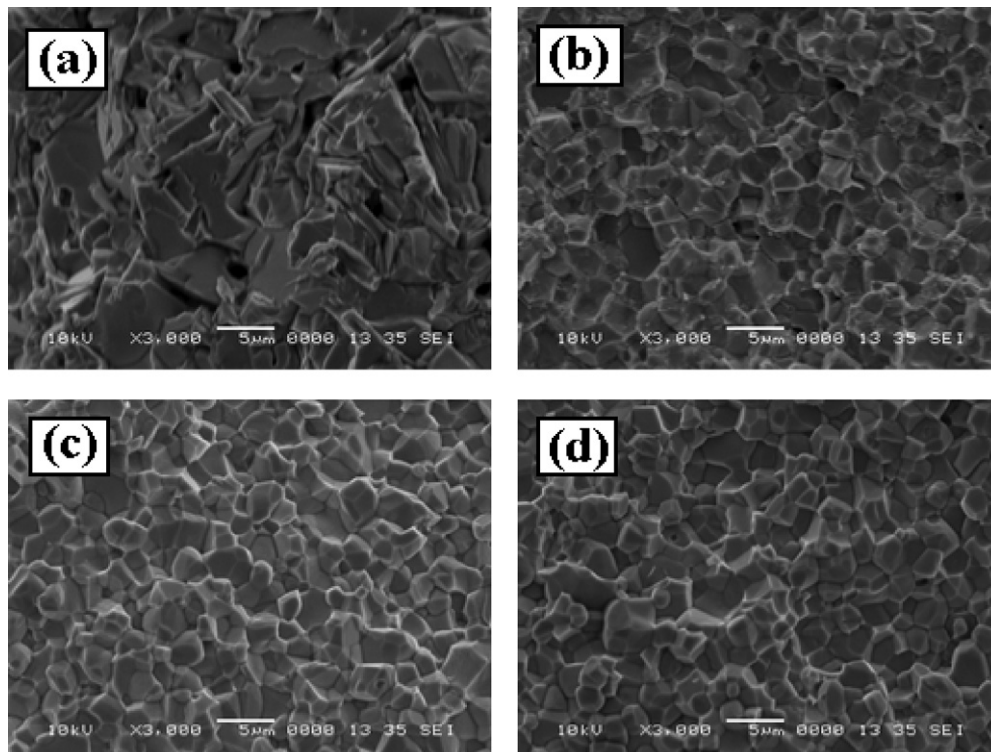


Fig. 3. Cross-section SEM images of the  $\text{SrO}(\text{Sr}_{0.5}\text{Ba}_{0.5}\text{TiO}_3)_n$  ceramics: (a)  $n = 1$ , (b)  $n = 2$ , (c)  $n = 3$  and (d)  $n = 4$ .

Table 1  
Dielectric properties of the  $\text{SrO}(\text{Sr}_{1-x}\text{Ba}_x\text{TiO}_3)_n$  ( $x = 0$  and  $0.5$ ,  $n = 1-4$ ) ceramics.

Samples	Tunability (30 kV/cm) (%)		Resonant frequency (GHz)	$\varepsilon$	$Q$ value
	at $-150^\circ\text{C}$	at $-100^\circ\text{C}$			
$x = 0.0, n = 1$	–	–	6.531	32.6	1963
$x = 0.0, n = 2$	–	–	3.448	59.2	1359
$x = 0.0, n = 3$	–	–	3.214	79.1	1290
$x = 0.0, n = 4$	11.35	6.49	2.519	102.3	1126
$x = 0.5, n = 1$	–	–	6.733	39.9	383
$x = 0.5, n = 2$	–	–	4.518	86.5	495
$x = 0.5, n = 3$	6.05	3.75	4.034	145.5	853
$x = 0.5, n = 4$	23.61	5.27	3.157	210.4	553

polarizability dominates permittivity [23]. As  $n$  increases, the SrO content decreases, so that average ionic polarizability increases, thus increasing permittivity [14]. The intrinsic loss strongly depends on permittivity [24]. The  $Q$  values of our samples are lower than those reported by Wise et al. [14], which may be related to the purity of raw materials, and second phases and porosity of the ceramics. Compared to that of  $\text{SrO}(\text{SrTiO}_3)_n$ , permittivity of the  $\text{SrO}(\text{Sr}_{0.5}\text{Ba}_{0.5}\text{TiO}_3)_n$  ceramics is higher, whereas their  $Q$  values are markedly lower. Because the

polarizability of  $\text{Ba}^{2+}$  ( $1.55 \times 10^{-30} \text{ m}^3$ ) is higher than that of  $\text{Sr}^{2+}$  ( $0.864 \times 10^{-30} \text{ m}^3$ ) [25],  $\text{Ba}^{2+}$  substitution for  $\text{Sr}^{2+}$  causes an increase in permittivity. The low  $Q$  value of the  $\text{SrO}(\text{Sr}_{0.5}\text{Ba}_{0.5}\text{TiO}_3)_n$  series is probably attributed to the formation of the  $\text{Ba}_x\text{Sr}_{2-x}\text{TiO}_4$  phase.

#### 4. Conclusions

For  $\text{SrO}(\text{SrTiO}_3)_n$  series,  $\text{Sr}_2\text{TiO}_4$  was single phase, while  $\text{Sr}_3\text{Ti}_2\text{O}_7$  and  $\text{Sr}_4\text{Ti}_3\text{O}_{10}$  were not single phase.  $\text{Sr}_4\text{Ti}_3\text{O}_{10}$  appeared in the samples with  $n \geq 2$  as either a major phase ( $n = 3, 4$ ) or a second phase ( $n = 2$ ).  $\text{SrTiO}_3$  appeared in the sample with  $n = 3$  and its amount increased as  $n$  increased.  $\text{Ba}^{2+}$  substitution for  $\text{Sr}^{2+}$  caused the formation of  $\text{SrTiO}_3$  and  $\text{Ba}_x\text{Sr}_{2-x}\text{TiO}_4$ . Meanwhile, it promoted the formation of equiaxed grains instead of block-like ones.  $\text{SrO}(\text{Sr}_{1-x}\text{Ba}_x\text{TiO}_3)_n$  ( $n = 1, 2$ ) had no tunability over  $-165$  to  $50^\circ\text{C}$ . As  $n$  increased, the tunability increased. Compared to  $\text{SrO}(\text{SrTiO}_3)_n$  series,  $\text{SrO}(\text{Sr}_{0.5}\text{Ba}_{0.5}\text{TiO}_3)_n$  series had higher permittivity and higher tunability, but lower  $Q$  value.

#### Acknowledgements

This research was supported by Zhejiang Provincial Science Foundation (No. Y6110475) and the undergraduate innovative project of Zhejiang Province (No. 2010R409016).

#### References

- [1] S. Ruddlesden, P. Popper, Acta Cryst. 10 (8) (1957) 538–539.
- [2] S. Ruddlesden, P. Popper, Acta Cryst. 11 (1) (1958) 54–55.
- [3] P. Balaya, M. Ahrens, L. Kienle, J. Maier, B. Rahmati, S.B. Lee, W. Sigle, A. Pashkin, C. Kuntscher, M. Dressel, J. Am. Ceram. Soc. 89 (9) (2006) 2804–2811.
- [4] Y. Hu, O. Tan, J. Pan, H. Huang, W. Cao, Sens. Actuators B: Chem. 108 (1–2) (2005) 244–249.
- [5] S. Burnside, J.E. Moser, K. Brooks, M. Grätzel, D. Cahen, J. Phys. Chem. B 103 (43) (1999) 9328–9332.
- [6] J. Li, S. Luo, M. Alim, Mater. Lett. 60 (6) (2006) 720–724.
- [7] J. Mateu, J.C. Booth, S.A. Schima, IEEE T. Microw. Theory 55 (2) (2007) 391–396.
- [8] M. Moreira, J. Andres, V. Longo, M. Li, J. Varela, E. Longo, Chem. Phys. Lett. 473 (4–6) (2009) 293–298.
- [9] X. Zhang, K. Huo, L. Hu, Z. Wu, P.K. Chu, J. Am. Ceram. Soc. 93 (9) (2010) 2771–2778.

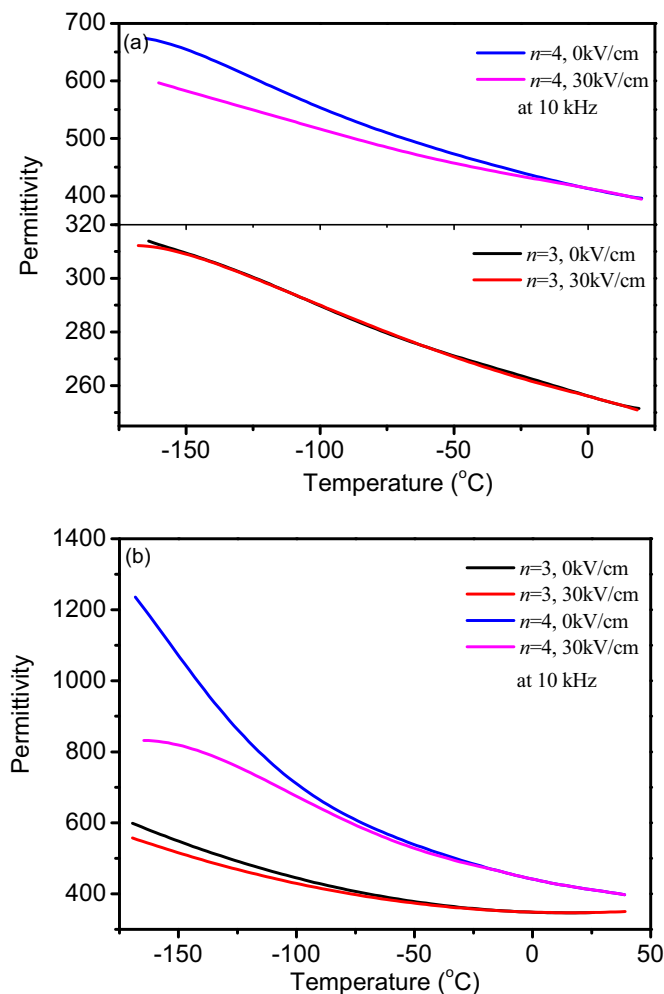


Fig. 4. Temperature dependences of permittivity of the  $\text{SrO}(\text{Sr}_{1-x}\text{Ba}_x\text{TiO}_3)_n$  ( $x = 0.0$  and  $0.5$ ,  $n = 3, 4$ ) ceramics: (a)  $x = 0.0$  and (b)  $x = 0.5$ .

- [10] T. Xian, H. Yang, J.F. Dai, Z.Q. Wei, J.Y. Ma, W.J. Feng, *Mater. Lett.* 65 (21–22) (2011) 3254–3257.
- [11] J. Haeni, P. Irvin, W. Chang, R. Uecker, P. Reiche, Y. Li, S. Choudhury, W. Tian, M. Hawley, B. Craigo, *Nature* 430 (7001) (2004) 758–761.
- [12] J. Haeni, *Appl. Phys. Lett.* 78 (21) (2001) 3292.
- [13] N. Zhou, G. Chen, H. Zhang, C. Zhou, *J. Alloys Compd.* 477 (1–2) (2009) L17–L20.
- [14] P. Wise, I. Reaney, W. Lee, T. Price, D. Iddles, D. Cannell, *J. Eur. Ceram. Soc.* 21 (10–11) (2001) 1723–1726.
- [15] N. Orloff, W. Tian, C. Fennie, C. Lee, D. Gu, J. Mateu, X. Xi, K. Rabe, D. Schlom, I. Takeuchi, *Appl. Phys. Lett.* 94 (2009) 042908.
- [16] B.W. Hakki, P.D. Coleman, *I.R.E Trans, Microw. Theory Tech.* 8 (1960) 402.
- [17] T. Hungria, A. Castro, *J. Alloys Compd.* 436 (1–2) (2007) 266–271.
- [18] K.H. Lee, Y.F. Wang, S.W. Kim, H. Ohta, K. Koumoto, *Int. J. Appl. Ceram. Technol.* 4 (4) (2007) 326–331.
- [19] Y.F. Wang, K.H. Lee, H. Ohta, K. Koumoto, *Ceram. Int.* 34 (4) (2008) 849–852.
- [20] Y. Wang, K.H. Lee, H. Hyuga, H. Kita, H. Ohta, K. Koumoto, *J. Electroceram.* 24 (2) (2010) 76–82.
- [21] X. Wang, H.L.-W. Chan, C.-L. Choy, *J. Am. Ceram. Soc.* 86 (10) (2003) 1809–1811.
- [22] J. Zhang, J. Zhai, X. Chou, J. Shao, X. Lu, X. Yao, *Acta Mater.* 57 (15) (2009) 4491–4499.
- [23] I.M. Reaney, I. David, *J. Am. Ceram. Soc.* 89 (7) (2006) 2063–2072.
- [24] R. Zurmuhlen, J. Petzelt, S. Kamba, G. Kozlov, A. Volkov, B. Gorshunov, D. Dube, A. Tagantsev, N. Setter, *J. Appl. Phys.* 77 (10) (1995) 5351–5364.
- [25] L. Pauling, *Proc. Roy. Soc. A* 114 (1927) 191.